GEOFIZIKA VOL. 25 No. 1 2008

Original scientific paper
UDC 550.34

Source parameters of the significant earthquakes in Egypt, 1992–1998 inferred from the P-waves magnitude spectra of teleseismic seismograms

H. M. Hussein and K. M. Abou Elenean

Seismology Department, National Research Institute of Astronomy and Geophysics, Egypt

Received 3 September 2007, in final form 5 March 2008

Using the P-wave magnitude spectra of the vertical component of teleseismic broadband seismograms, average source parameters have been retrieved for five significant earthquakes of $M_w \geq 5.7$ occurring in Egypt namely, 1992 Cairo earthquake, 1998 Alexandria earthquake and three events which occurred in the Gulf of Aqaba region between 1993 and 1995. The magnitude spectrum represents the velocity amplitude density spectrum at the earthquake source, scaled in magnitude units. The maximum of the magnitude spectrum along with the period at which the maximum occurs are used to estimate the source parameters. For precise determination of the source parameters, two different methods for deriving the corner periods are applied. The obtained source parameters were compared with those derived in previous studies. The results show that within the moment magnitude range 5.5 ~ 7.2, the corner periods are 1.29 ~ 11.6 s, length of the fault ruptures are 5.5 ~ 50 km and the stress drops are 0.5 ~ 4.8 MPa. The derived stress drop shows an increasing trend with the seismic moment for the three Gulf of Aqaba earthquakes. The 1995 Gulf of Aqaba earthquake of $M_w = 7.2$, the largest earthquake to have occurred in Egypt in the last century is characterized by a higher complexity compared to the other events, that are much simpler. The values of the corner periods for this earthquake are azimuth dependent due to complexity and strong directivity of its rupture. For a detailed description of the complexity of 1995 earthquake additional source parameters are also estimated in terms of an inhomogeneous source model. These parameters are the asperity radius, displacement across the asperity, localized stress drop and ambient faulting stress. The average stress drop of Cairo, 1992 and Alexandria, 1998 intraplate earthquakes shows larger values compared with the interplate 1993 Gulf of Aqaba earthquakes. Generally, the estimated seismic moment using the magnitude spectra reflect good agreement with the estimates made from the other techniques for simple source while the complex source yields smaller values.

Keywords: magnitude spectra, source parameters, source complexity

1. Introduction

Egypt lies on the northeast corner of the African continent and is bounded by three active tectonic margins (Figure 1, inset): the African-Eurasian plate margin (convergent margin); the Red Sea plate margin (rifting margin); the Levant-Dead Sea transform fault (left lateral strike slip movement). The major part of tectonic deformation is remote and took place along the mentioned three margins as revealed by an observed highest rate of seismic activity. Meanwhile, a part of the deformation is transferred to the land to rejuvenate some of the pre-existing NW–SE, WNW–ESE, E–W and WSW–ENE faults with predominant normal faulting with slight shear component (Abou Elenean, 2007). Generally, the inland seismic activity has moderate sizes while the plate margins earthquakes have large sizes. A dominant tensile stress oriented NE–SW to ENE–WSW prevailed at the NE corner of Africa along the Northern Red Sea-Gulf of Suez-Gulf of Aqaba rifts while it is oriented NNE–SSW on the Egyptian land. Towards the Mediterranean Sea the dominant inland tension changes to a dominant compression along the transition zone between the continental-oceanic crusts. This change indicates an extension of the back thrusting effect and/or positive inversion of the previous passive margin due to the subduction of the African plate under the Eurasian plate (Abou Elenean and Hussein, 2007).

Recently, five significant earthquakes ($M_w \geq 5.7$) struck Egypt that is the 1992 Cairo earthquake, the 1993 and 1995 three Gulf of Aqaba earthquakes and the 1998 Alexandria earthquake (Figure 1). The parameters of these earthquakes are listed in Table 1. These events were recorded teleseismically by several broadband stations which provide detailed basic data to investigate the features of the source properties. The 1995 Gulf of Aqaba is the strongest event ($M_w = 7.2$) in Egypt since the 1969 Shedwan Island earthquake while the 1992 Cairo earthquake is the one which caused severe damage compared to the others. These events have been investigated based on the moment tensor inversion of the teleseismic records (Hussein, 1999) and spectral analysis of teleseismic P waves (Hussein et al., 1998). Regional broadband data was also used for the moment tensor and source parameters estimation for the 1998 Alexandria earthquake (Abou Elenean and Hussein, 2007). Harvard University reports the centroid moment tensor (CMT) inversion solutions for these events, in addition to their seismic moments. All of the five shocks occurred at a shallow depth from 9 to 22 km; the 22 km depth Cairo event is the deepest one. The three studied Gulf of Aqaba earthquakes are the third of August 1993 event (12:43), its largest aftershock (16:33) and the November 22, 1995 event. The 1995 earthquake was the largest shock to occur along the Aqaba-Dead Sea Transform fault in at least a century. Although it was the largest one to struck Egypt, minor damage has occurred due to the sparse population density along the Gulf of Aqaba region. The estimated source parameters collected from the previous studies are listed in Table 2.

Table 1. Parameters of the studied events.

Event no.	Date	O. Time	Lat.	Lon.	Depth	m_b(ISC)	M_w
1	19921012	130955	29.76	31.14	22	5.8	5.8
2	19930803	124305	28.78	34.57	10	5.8	6.1
3	19930803	163321	28.79	34.59	13	5.4	5.7
4	19951122	041511	28.81	34.80	09	6.1	7.2
5	19980528	183328	31.45	27.64	10	5.5	5.5

Table 2. Source parameters of the studied events estimated in the previous work.

Studied Events	M_0 (Nm)	L (km)	D (m)	$\Delta\sigma$ (MPa)	References
19921012	5.5×10^{17}				CMT
		11	0.24	1.85	Hussein (1999)
19930803(12:43)	12.3×10^{17}		0.25	0.8	Hussein et al. (1998)
	14×10^{17}			3.5	Pinar and Turkelli (1997)
	17.6×10^{17}				CMT
				0.88	Abdel Fattah (1996)
19930803(16:33)	2.2×10^{17}		0.09	0.3	Hussein et al. (1998)
19951122	30×10^{18}		1.05	2.47	Abdel Fattah et al.(2006)
	34×10^{18}	50	0.9	2	Pinar and Turkelli (1997)
		65			Baer et al. (2002)
19980528	1.98×10^{17}				CMT
	1.24×10^{17}		0.13	0.7	Abou Elenean and Hussein (2007)

In the present study, we first determine the source parameters of these earthquakes from the teleseismic records using the P-wave magnitude spectra and then compare the derived source parameters with those determined using moment tensor inversion of regional and teleseismic broadband seismograms and P-wave spectral analysis of the broadband teleseismic waveforms. Moreover, individual features related to rupture complexities and the radiation process at the hypocenters are assigned. As described by Sarkar and Duda (1985) and Kaiser et al. (1996), the spectral magnitude for P-waves is computed by applying a set of non overlapping band pass filters to the broadband records in order to obtain band pass seismograms from which P wave magnitude of a certain earthquake can be calculated at different frequencies. Narrowing the passband to the resolvable frequency chosen for the Fourier transform, i.e. admitting only one Fourier component to each passband, yields a sequence of magnitudes which will constitute the P-wave magnitude spectrum of the given

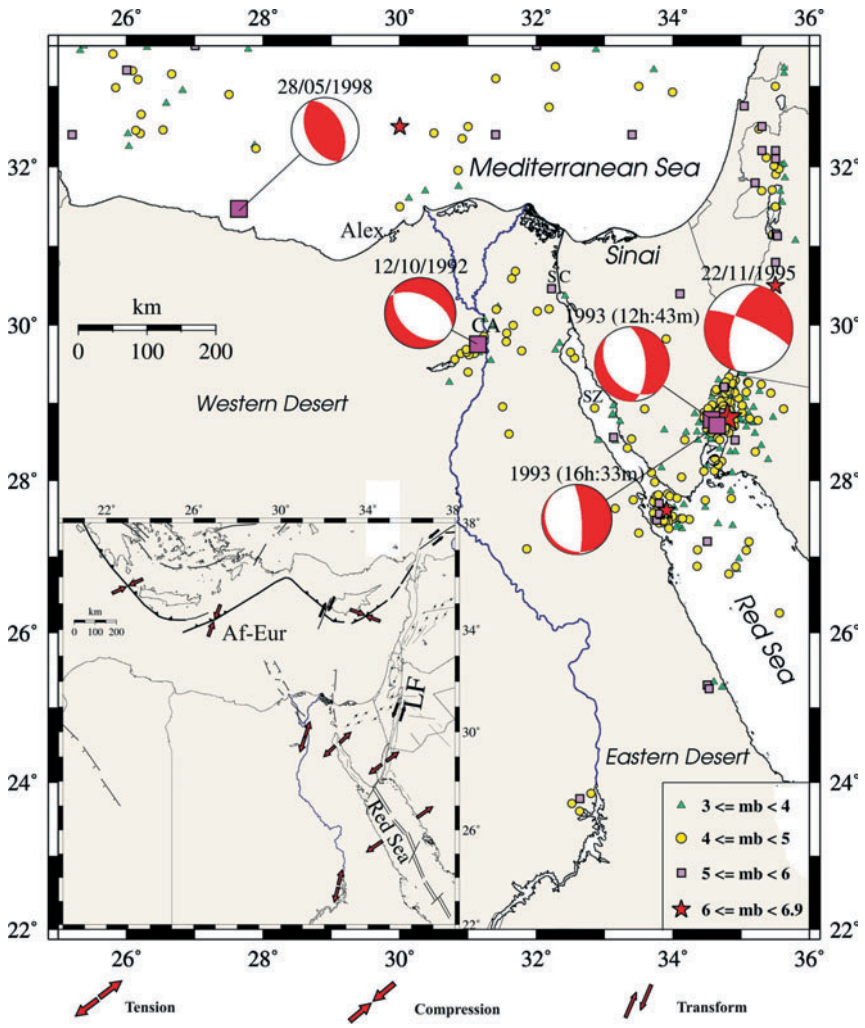

Figure 1. Location map of the studied five significant earthquakes (larger symbols) which occurred from 1992 to 1998 (marked by their CMT focal mechanisms). Seismicity data (mb ≥ 3) was complied after: Riad and Meyers, 1985 (1900 to 1964); ISC (1964–2005). Acronyms: AQ, Gulf of Aqaba; LF, Levant Fault; Af-Eur, African-Eurasian plate margin; SC, Suez Canal; SZ, Gulf of Suez; Alex, Alexandria; CA, Cairo. Tectonic boundaries of Egypt (Abou Elenean and Hussein, 2007) are shown on the inset map.

earthquake. In order to compensate for the propagation losses, the frequency-dependent magnitude calibration function (Nortmann and Duda, 1983) is employed. The maximum spectral magnitude together with the period at which it occurs are thereby the most characteristic quantities of the radiated spectrum and more representative of the strength of the earthquake than the

conventional body wave magnitudes. Accurate source parameters for the studied five events are useful for hazard evaluation in Egypt that represents a heavily populated area.

2. Data analysis

In this analysis, we have used the teleseismic records of the recent significant earthquakes in Egypt from IRIS broadband stations, which are located at epicentral distances in the range 15° to 90° and have different azimuths. Choice of the records is mainly based on clarity of the records and low noise level. The locations of the events analyzed in this study are shown in Figure (1) and their parameters are listed in Table 1. The records were instrumentally corrected prior to processing. The magnitude spectra for each individual record of the five earthquakes were computed by applying the PASTA program developed by Roslov (1994) to a time window length of 60 seconds, started 5 seconds before the P wave onset. The window length was selected to be at least six times the corner period to yield stable value of the corner period (Kaiser and Duda, 1988). A 10% cosine tapering window is applied at both ends of the signal. Adopting the analysis technique of P wave magnitude spectra for ground motion velocity, we have estimated the source parameters, such as seismic moment, corner frequency, fault length and seismic stress drop in addition to the source complexity. The average values of source parameters are obtained by averaging the derived values from the individual stations of each earthquake. For the evaluation of the uncertainties in the estimated source parameters, we calculate the standard errors of the sample average or mean and the standard deviations in these parameters at the various stations.

3. Determination of source parameters

For estimating the source parameter, we followed the method developed by Kaiser and Duda (1988), Kaiser (1989), and Kaiser et al. (1996) which we briefly summarize here. The maximum of the magnitude spectrum $(m_f)_{\max}$ and the corresponding period T_0 is related to the seismic moment, M_0 for the omega-square model through the relation:

$$M_0 = 10^{(m_f)_{\max} - 0.7} T_0 \left[\frac{2\rho_r c_r {c_s}^4}{\pi {R_{\theta\phi}}^2} \right]^{1/2} \tag{1}$$

where $\rho_r = 2720$ kg m^{-3} is the density near the receiver, c_r and c_s are the velocities of the P wave near the receiver and the source and assumed to be 5800 m/s and 6100 m/s, respectively. $R_{\theta\phi}$ is the average radiation pattern coefficient for P-wave and a mean value of 0.44 is used (Boore and Boatwright, 1984). The values of T_0 is also used to calculate the focal parameters, such as a_0 (fault ra-

dius), L (fault length) and $\Delta\sigma$ (stress drop). Using the Brune (1970, 1971) model the relation between T_0 and a_0 is:

$$a_0 = 0.37\, c_s T_0 \tag{2a}$$

Considering the approximation that the fault length equals to $2a_0$, the fault length can be expressed as:

$$L = 0.74\, c_s T_0 \tag{2b}$$

The average static stress drop is:

$$\Delta\sigma = \frac{7}{16}\frac{M_0}{{a_0}^3} \tag{3}$$

(Keilis-Borok, 1959) and the average displacement D_0 over a circular fault area is obtained from the equation:

$$D_0 = \frac{M_0}{\pi {a_0}^2 \mu} \tag{4}$$

(Brune, 1968) where $\mu = 2.7 \times 10^{10}$ Pa expresses the shear modulus of the fault material.

Visual inspection of T_0 over the magnitude spectra observation is a kind of easy method for a simple rupture earthquake. However, an earthquake with a complex rupture process generally has a broad and complicated spectrum with secondary maxima at periods shorter or longer than T_0, at which the maximum magnitude $(m_f)_{max}$ occurs. The difficulty in determining the corner periods for such spectra have been discussed by Madariaga (1979) and Boatwright (1984). Following Duda and Kaiser (1989), another two different measures of the corner periods are utilized in the present study. The first, T_c, corresponds to the location of the first moment of the energy density spectrum. Furthermore, T_c represents a weighted average value in case of complex spectra with several maxima. The weight of each corner period depends on the energy carried in the respective maximum. Thus, T_c is preferred over T_0 and can be calculated as:

$$T_c = \frac{E_p}{\int_0^\infty E_P(f) f df} \tag{5}$$

where E_P is the total P-wave energy radiated from the earthquake focus and is given by:

$$E_P = \int_0^\infty E_P(f) df \tag{6}$$

Whereas $E_P(f)$ is P-wave energy density spectrum (J/Hz) which is related to the magnitude spectrum $m(f)$ through the relation:

$$E_P(f) = 10^{2m(f)-14} \tag{7}$$

For estimating the source parameters T_0 is replaced by T_c in equation (2a) and (2b). Boatwright (1980), Hanks (1982) and Andrews (1986) pointed out that T_c has a higher stability than T_0 because it results from integration of the spectrum. The instability of T_0 could be related to the site effect specially for small to moderate size earthquakes that have smaller corner periods closer to the receiving sites amplification periods. This phenomenon could lead to the existence of several maxima and difficulties in assigning the exact T_0 value. Nevertheless, most larger earthquakes with larger corner periods have identical T_0 and T_c (Kaiser et al., 1996).

The second measure, the corner period T_S was proposed by Snoke (1987) and Duda and Kaiser (1989) and is given by:

$$T_S = \frac{\pi R_{\theta\phi} 10^{(m_f)_{\max}-1.4}}{E_P} \tag{8}$$

T_S in equation (8) is the corner period of the P wave magnitude spectrum with total P wave energy E_P and with maximum magnitude $m_f(max)$ as determined from the observed spectrum (Kaiser et al., 1996), but with a shape corresponding to the omega-square spectrum for the P wave (Aki, 1967; Brune, 1970). In case of complex rupture, the observed spectrum is not consistent with the omega-square source model. Therefore, T_S underestimates the corner period in these cases (Boatwright, 1984). The ratio T_c / T_S can be used as a measure of rupture complexity (Duda and Kaiser, 1989; Kaiser et al., 1996). However, T_c is independent on the source model in contrary to T_S. The rupture complexity C is defined as

$$C = T_C / T_S \tag{9}$$

In practice, the values of complexity C for intermediate and large earthquakes are in the range of 0.5 to 2.5 (Kaiser, 1989). For $C < 0.8$, the source is considered to be homogenous. Assuming an inhomogeneous fault model (McGarr, 1981), asperity radius a_i surrounded by previously faulted annular region of outer radius a_0 can be deduced from the complexity value C as:

$$\frac{a_0}{a_i} = 5.7(4C - 3) \tag{10}$$

Equation (10) is based on the assumption that an annular region $a_i < a < a_0$ has failed under the influence of an ambient fault stress σ_{af} in either preceding the earthquake or in aseismic creep. σ_{af} represents the difference between the

regional applied shear stress and the frictional stress that resist sliding across the fault zone. Essentially, the asperity fails with a high stress drop $\Delta\sigma_i$ that is many times larger than the average stress drop $\Delta\sigma$ throughout the total zone of faulting. The source parameters of the small dimension failure can be determined according to McGarr (1981). The small scale stress drop $\Delta\sigma_i$ is

$$\Delta\sigma_i = \frac{2}{3}\Delta\sigma\left(\frac{a_0}{a_i}\right)^2 \tag{11}$$

and the corresponding average displacement owing to the failure of asperity is

$$D_i = \frac{1.52}{\pi}\frac{\Delta\sigma}{\mu}\frac{{a_0}^2}{a_i} \tag{12}$$

While the ambient fault stress σ_{af} is given by

$$\sigma_{af} = \frac{2}{3}\Delta\sigma\frac{a_0}{a_i}\left[1 + 0.06\frac{a_i}{a_0} + 0.33\left[\frac{a_i}{a_0}\right]^2 + 0.04\left[\frac{a_i}{a_0}\right]^3\right] \tag{13}$$

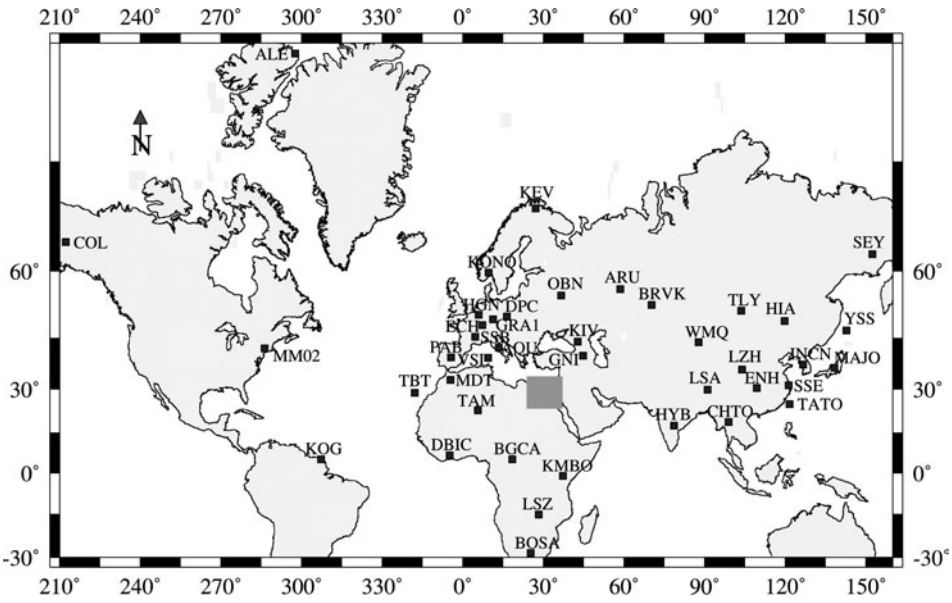

Figure 2. Broadband seismic stations used for calculating the magnitude spectra for the studied earthquakes. Symbols are annotated by the international station codes. Studied area is enclosed by shaded square.

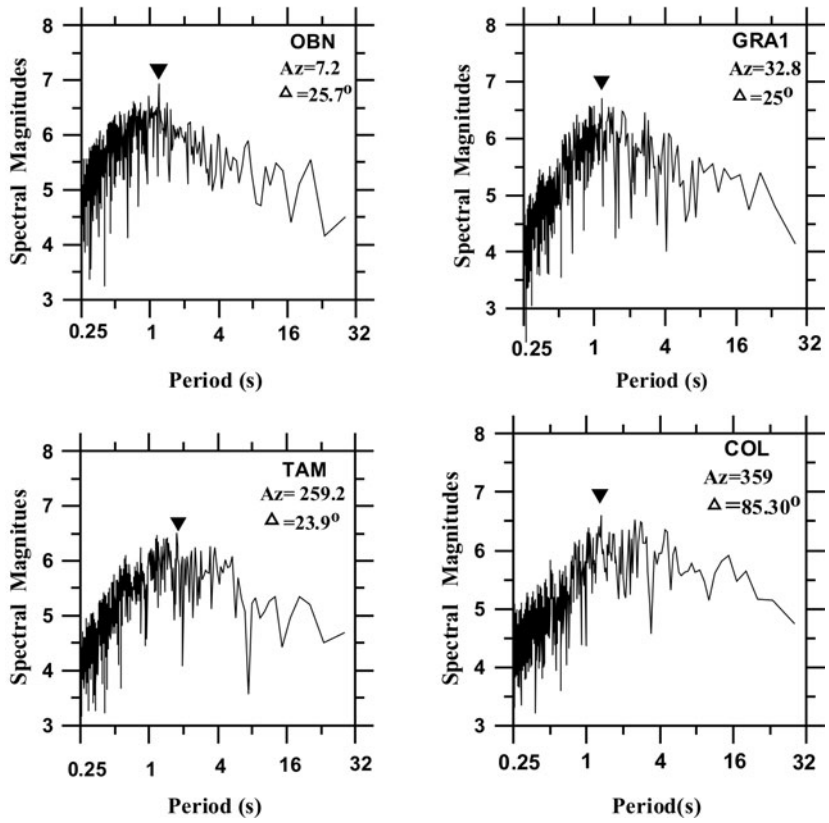

Figure 3. P-wave magnitude spectra of the October12, 1992 Cairo earthquake. Corner periods are marked by inverted triangle. Text attached with each plot indicate station code, azimuth and epicentral distance.

The standard error (SE) of the mean for the estimated source parameters at different stations can be computed by the formula of Zwillinger (1995),

$$SE = \frac{S}{\sqrt{N}} \tag{14}$$

where S is the slandered deviation and N is the number of the source parameter data.

4. Interpretation of the magnitude spectra

Based upon the magnitude spectra of available broadband stations (Figure 2), the source parameters of five significant events are estimated:

(1) The earthquake of October 12, 1992 (13h:09m)

Magnitude spectra for this event from thirteen broadband stations with different azimuths are estimated. The spectral shape for this earthquake is very similar at the processed thirteen stations. An example of the magnitude spectra at four stations with different azimuths are shown in Figure (3). The estimated source parameters based on both T_0 and T_c for this event are listed in Tables 3 and 4. Due to the advantages of using T_c, the calculated average seismic moment is 4.4×10^{17} Nm, somewhat consistent with the value of 5.5×10^{17} Nm of CMT. Meanwhile the seismic moment determined from T_0 (2.16×10^{17} Nm) is nearly half the CMT value. The average stress drop, average fault length and average dislocation derived using T_c are 1.55 MPa, 10.63 km and 0.2 m, respectively. These source parameters are almost identical to those found from the inversion of teleseismic body wave by Hussein (1999)

Table 3. Estimated average spectral magnitude, maximum observed spectral magnitude, corner periods T_0, T_c, T_s and the rupture complexity of Cairo 1992 earthquake.

St. Code	Az.	Δ°	Aver. m_f	m_f	E_p (10^{11} J)	T_0 (sec)	T_C (sec)	T_S (sec)	C
OBN	07.2	25.7	6.10	6.94	7.07	1.19	1.71	6.89	0.24
KIV	29.7	16.9	5.78	6.59	1.29	1.33	2.73	7.65	0.36
GRA1	32.8	25.0	5.88	6.72	2.24	1.16	2.12	8.00	0.27
GNI	43.3	15.2	6.00	6.73	2.40	1.11	2.48	7.83	0.31
HIA	45.1	67.1	5.62	6.39	0.70	1.40	2.50	5.63	0.44
MAJO	50.5	84.8	5.89	6.63	2.27	1.32	3.08	5.21	0.53
LSA	74.1	51.1	5.52	6.19	0.26	0.83	2.79	5.88	0.47
HYB	94.9	44.8	5.63	6.24	0.67	1.35	2.45	2.29	1.06
TAM	259.2	23.9	5.80	6.50	1.50	1.73	2.47	4.33	0.57
SSB	314.0	26.0	5.65	6.42	0.68	1.50	3.07	6.65	0.46
ECH	321.0	26.0	5.71	6.48	0.62	1.28	2.65	9.06	0.27
KONO	340.2	33.0	5.76	6.59	1.89	1.20	2.44	5.19	0.47
COL	359.0	85.3	6.03	6.61	2.06	1.31	3.13	5.22	0.60
Aver.			5.80 ±	6.54 ±	1.82 ±	1.29 ±	2.58 ±	6.14 ±	0.47 ±
SE			0.05	0.06	0.47	0.06	0.11	0.49	0.05
S.D.			0.18	0.20	1.74	0.21	0.40	1.80	0.21

St., stations code; Δ°, epicentral distance in degrees; Aver. m_f, maximum average spectral magnitude over one octave; m_f, maximum calculated spectral magnitude; E_p, released seismic energy (J); T_0, corner period corresponding to the observed maximum spectral magnitude; T_C, corner period corresponding to the location of the first moment of the energy density spectrum; T_S, defined by eq. 9; C, rupture complexity; SE is the standard error of the mean. S.D. is the value of the standard deviation.

Table 4. Source parameters derived from T_0 nd T_C of Cairo 1992 earthquake.

St. Code	Parameters based on T_0				Parameters based on T_C			
	M_0 (10^{17} Nm)	L (km)	D (m)	$\Delta\sigma$ (MPa)	M_0 (10^{17} Nm)	L (km)	D (m)	$\Delta\sigma$ (MPa)
OBN	1.82	5.11	0.33	04.87	07.37	7.34	0.65	6.50
KIV	2.56	5.71	0.37	04.82	05.25	5.86	0.18	1.14
GRA1	3.01	4.98	0.57	08.54	05.51	9.09	0.31	2.55
GNI	2.95	4.76	0.61	09.55	06.46	10.43	0.28	1.99
HIA	1.70	6.00	0.22	02.74	03.03	10.73	0.12	0.86
MAJO	2.79	5.67	0.41	05.36	06.50	13.21	0.18	0.99
LSA	0.63	3.56	0.24	04.90	02.14	11.97	0.07	0.44
HYB	1.16	5.79	0.16	02.09	02.11	10.51	0.09	0.63
TAM	2.71	7.43	0.23	02.13	03.86	10.60	0.16	1.13
SSB	1.95	6.44	0.22	02.56	04.00	13.17	0.11	0.61
ECH	1.90	5.59	0.29	04.00	03.90	11.37	0.14	0.94
KONO	2.30	5.15	0.40	05.90	04.69	10.47	0.20	1.43
COL	2.64	5.62	0.39	05.19	06.31	13.43	0.16	0.91
Aver.	2.16	5.52	0.34	4.81	4.70	10.63	0.20	1.55
	±	±	±	±	±	±	±	±
SE	0.19	0.25	0.04	0.62	0.46	0.60	0.04	0.43
S.D.	0.72	0.91	0.14	2.28	1.71	2.20	0.15	1.60

M_0, seismic moment; L, total fault length; D, dislocation; $\Delta\sigma$, stress drop; SE is the standard error of the mean; S.D. is the value of the standard deviation.

which gives stress drop, fault length and average dislocation of 1.85 MPa, 11 km and 0.24 m respectively. The estimated complexity value is 0.47 which reflects a homogenous source.

(2) The earthquake of August 3, 1993 (12h:43m)

The source parameters for this event are calculated based upon the magnitude spectrum of twelve broadband stations. The magnitude spectra are quite similar at the processed stations as shown in Figure 4. Tables 5 and 6 list the source parameters for each individual station in addition to the average value of each parameter. The seismic moment is 11.27×10^{17} Nm based on T_c value that is almost identical with 12.3×10^{17} Nm value obtained by Hussein et al. (1998) and is quite consistent with the seismic moment of 14×10^{17} Nm estimated using body waveform inversion obtained by Pinar and Turkelli (1997) but is relatively lower than the value of 17.60×10^{17} Nm obtained by HRVD.

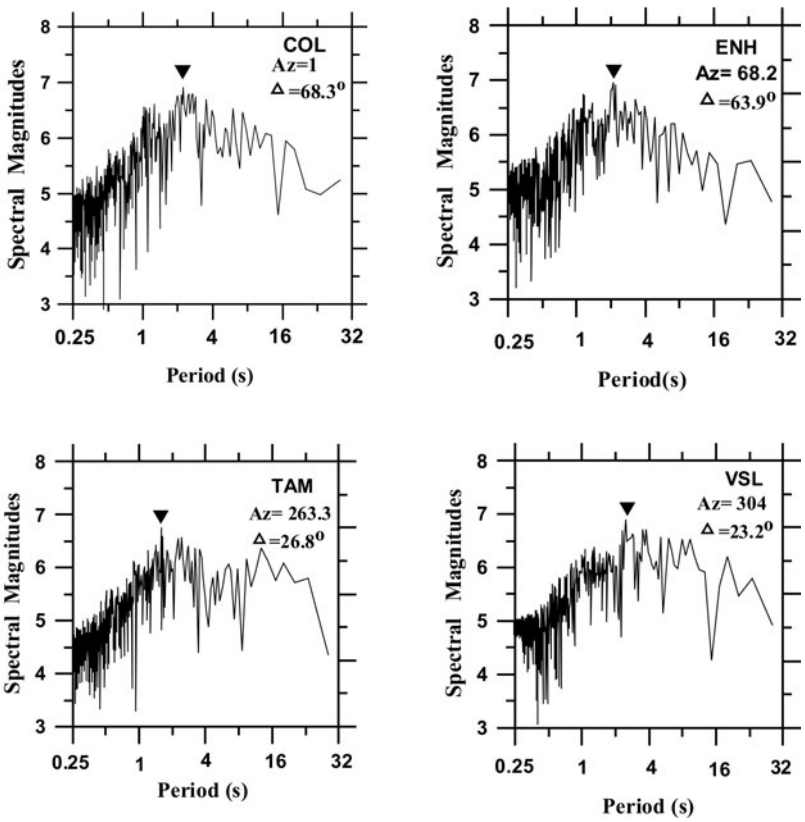

Figure 4. P-wave magnitude spectra for the August 3, 1993(12h:43m) Gulf of Aqaba earthquake. Plot parameters are similar to Figure (3).

The seismic moment estimated from T_0 is 6.25×10^{17} Nm which is about 2–3 times smaller than the seismic moments estimated by the different methods. The others source parameters computed from the corner period T_c are the stress drop, 1.08 MPa, fault length, 15.69 km and dislocation, 0.22 m. Using the spectral analysis of regional waveform (Abdel Fattah, 1996) and teleseismic waveform (Hussein et al., 1998) the calculated stress drop are 0.88 and 0.8 MPa, respectively. These values are in reasonable agreement with our estimate, whereas the stress drop inferred by Pinar and Turkelli (1997) is about 3 times larger than the value obtained in this study (3.5 MPa). This relatively larger value is roughly estimated from the moment and only the area of the major slip. The estimated dislocation from the teleseismic waveform inversion (Pinar and Turkelli, 1997) is about 0.25 m which is quite similar to the value obtained in this study. The obtained value of the rupture complexity for this event is 0.64, reflecting a simple rupture source.

Table 5. Estimated average spectral magnitude, maximum observed spectral magnitude, corner periods T_0, T_c, T_s and the rupture complexity of the Gulf of Aqaba, 1993 (12:43) earthquake.

St. Code	Az.	Δ°	Aver. m_f	m_f	E_p (10^{11} J)	T_0 (sec)	T_C (sec)	T_S (sec)	C
COL	01.00	68.3	6.22	6.91	6.66	2.22	4.17	6.45	0.65
OBN	02.60	26.4	6.10	6.81	4.05	1.68	2.54	6.69	0.38
SEY	24.50	76.0	6.10	6.84	5.48	2.27	3.90	5.68	0.69
YSS	41.10	80.5	6.00	6.74	4.62	2.76	2.95	4.24	0.70
HIA	45.60	65.6	5.84	6.60	1.90	2.22	3.26	5.41	0.60
WMQ	55.40	44.2	6.10	6.74	6.25	2.13	3.13	3.41	1.00
SSE	63.40	73.0	6.10	6.89	5.33	2.09	4.12	7.35	0.56
ENH	68.20	63.9	6.10	6.97	6.32	2.08	3.48	8.96	0.39
TAM	263.8	26.8	6.00	6.75	2.03	1.57	3.64	10.11	0.36
VSL	304.0	23.2	6.20	6.80	5.10	2.50	4.70	5.07	0.93
DPC	332.0	25.0	5.90	6.57	1.38	2.49	4.31	6.48	0.66
ALE	351.0	62.4	6.10	6.65	2.90	2.13	3.50	4.46	0.78
Aver.			6.01	6.77	4.43	2.17	3.64	6.19	0.64
			±	±	±	±	±	±	±
SE			0.03	0.04	0.54	0.10	0.18	0.56	0.06
S.D.			0.11	0.12	1.86	0.33	0.62	1.94	0.20

Parameters symbols are as in Table 3.

(3) The earthquake of August 3, 1993 (16h:33m)

The magnitude spectra for the largest aftershock of the August 3, 1993 (12h:43m) main shock at two broadband stations are shown in Figure 5. Based on T_c at seven stations, the average seismic moment and dislocation are 2.03×10^{17} Nm and 0.07 m in good agreement with the values of 2.20×10^{17} Nm and 0.09 obtained from the P wave displacement spectra of the teleseismic seismograms (Hussein et al., 1998). Meanwhile the calculated average stress drop is 0.52 MPa which is about 1.5 times higher than 0.3 MPa value of Hussein et al. (1998). The estimated complexity for this event is 0.66 that indicates a simple uniform rupture. The average source parameters calculated in this study are listed in Tables 7 and 8.

(4) The earthquake of November 22, 1995 (4h:15m)

Being the largest recorded event in Egypt during the last century up to now for which seismic data from the global digital network are available at different azimuths, it provides an excellent opportunity to study its source pa-

Table 6. Source parameters derived from T_0 and T_C of the Gulf of Aqaba, 1993 (12:43) earthquake.

St. Code	Parameters based on T_0				Parameters based on T_C			
	M_0 (10^{17} Nm)	L (km)	D (m)	$\Delta\sigma$ (MPa)	M_0 (10^{17} Nm)	L (km)	D (m)	$\Delta\sigma$ (MPa)
COL	5.02	9.53	0.26	2.03	16.80	17.89	0.25	1.02
OBN	5.37	7.21	0.49	5.01	08.11	10.09	0.32	2.19
SEY	7.77	9.74	0.39	2.94	13.35	16.74	0.22	1.00
YSS	7.51	11.85	0.25	1.58	08.02	12.66	0.24	1.38
HIA	4.37	09.53	0.23	1.76	06.42	13.99	0.15	0.82
WMQ	5.79	09.14	0.33	2.65	08.50	13.43	0.22	1.23
SSE	8.03	08.97	0.47	3.89	15.83	17.68	0.24	1.00
ENH	9.61	08.93	0.57	4.72	17.73	16.48	0.31	1.39
TAM	4.37	06.74	0.45	5.00	10.12	15.62	0.20	0.92
VSL	7.81	10.73	0.32	2.21	14.67	20.17	0.17	0.63
DPC	4.58	10.69	0.17	1.31	07.92	18.50	0.11	0.44
ALE	4.71	09.14	0.27	2.16	07.74	15.02	0.16	0.88
Aver.	6.25	9.35	0.35	2.93	11.27	15.69	0.22	1.08
SE	± 0.50	± 0.41	± 0.04	± 0.40	± 1.19	± 0.82	± 0.02	± 0.13
S.D.	1.80	1.41	0.12	1.37	4.10	2.80	0.06	0.45

Parameters symbols are as in Table 4.

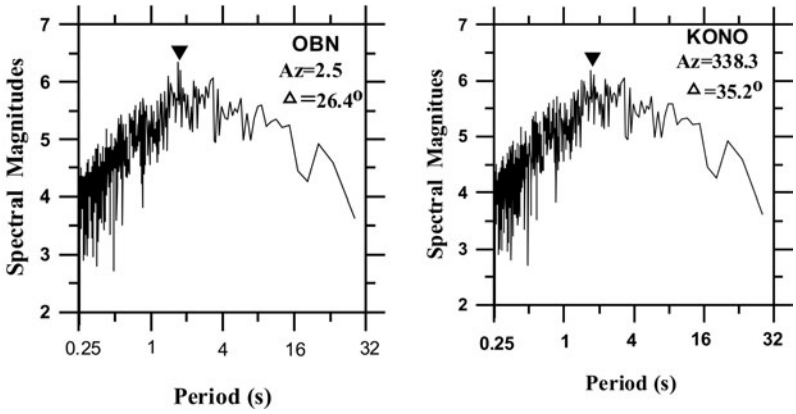

Figure 5. P-wave magnitude spectra for the August 3, 1993 (16h:33m) Gulf of Aqaba earthquake. Plot parameters are similar to Figure (3).

Table 7. Estimated average spectral magnitude, maximum observed spectral magnitude, corner periods T_o, T_c, T_s and the rupture complexity of the Gulf of Aqaba, 1993 (16:33) earthquake.

St. Code	Az.	D°	Aver. m_f	m_f	E_p (10^{11} J)	T_0 (sec)	T_C (sec)	T_S (sec)	C
OBN	02.50	26.40	5.70	6.48	6.89	1.50	2.01	8.61	0.24
KIV	20.90	16.50	5.12	5.94	9.66	1.68	2.78	5.11	0.54
ARU	24.80	32.40	5.36	6.20	2.84	1.33	2.11	5.75	0.37
CHTO	84.30	59.10	5.13	5.82	0.50	1.68	3.77	5.67	0.66
TBT	283.2	45.60	5.72	6.21	6.25	1.50	3.30	2.73	1.21
HGN	323.0	30.70	5.42	6.15	1.41	1.48	2.93	9.10	0.32
KONO	338.3	35.20	5.62	6.13	4.07	1.71	3.66	2.90	1.25
Aver.			5.43	6.13	4.50	1.55	2.93	5.07	0.66
± SE			± 0.09	± 0.08	± 1.34	± 0.06	± 0.29	± 1.01	± 0.17
S.D.			0.25	0.21	3.26	0.14	0.70	2.48	0.42

Parameters symbols are as in Table 3.

Table 8. Source parameters derived from T_0 and T_C of the Gulf of Aqaba, 1993 (16:33) earthquake.

Station	Parameters based on T_0				Parameters based on T_C			
	M_0 (10^{17} Nm)	L (km)	D (m)	$\Delta\sigma$ (MPa)	M_0 (10^{17} Nm)	L (km)	D (m)	$\Delta\sigma$ (MPa)
OBN	2.24	6.44	0.25	2.94	3.00	08.83	0.19	1.64
KIV	0.70	7.21	0.06	0.68	1.19	11.90	0.04	0.25
ARU	1.04	5.71	0.15	1.96	1.65	09.05	0.10	0.77
CHTO	0.55	7.21	0.05	0.51	1.23	16.18	0.02	0.10
TBT	1.20	6.43	0.14	1.57	2.65	07.08	0.06	0.33
HGN	1.03	6.35	0.12	1.41	2.05	12.57	0.06	0.36
KONO	1.14	7.34	0.10	1.01	2.44	15.07	0.04	0.22
Aver.	1.13	6.67	0.12	1.44	2.03	11.05	0.07	0.52
± SE	± 0.22	± 0.25	± 0.03	± 0.34	± 0.29	± 1.4	± 0.02	± 0.22
S.D.	0.54	0.60	0.07	0.83	0.71	3.38	0.06	0.54

Parameters symbols are as in Table 4.

rameters and the rupture process. The magnitude spectra of twenty three broadband stations are calculated and the estimated source parameters based on both T_0 and T_c are listed in Table 9. For this magnitude size, the observed corner periods at the processed stations are larger compared to the other events that in turn support that both T_0 and T_c are located away from the maxima related to the site effect. There is no significant variability in source parameters calculated from both T_0 and T_c compared to the other studied events. Inspection of the estimated T_0 and T_c indicates that their values are azimuthaly dependent. The stations on the northern size of the NNE trending Gulf of Aqaba have average corner periods (T_0) ~ 5.37 s which are smaller compared to the stations to the south of the gulf that have corner periods ~ 11.69 s. The focal mechanism of 1995 earthquake and its aftershocks distribution indicate N22°E left lateral strike slip fault with minor normal component (Hofstetter et al., 2003). The variation of the corner periods depending on the azimuth is interpreted as directivity effect. Rupture process study for the 1995 earthquake by Hofstetter et al. (2003) indicates a northward directivity effect for this event. The lower corner periods (higher frequencies) appear in the direction of the rupture propagation. Figure 6 shows the magnitude spectra for three stations at three different azimuths (ARU at N24°E, HYP at N96°E and BGCA at N216°E). Examining the observed magnitude spectra at theses stations, we note that the spectrum have a different shapes along different azimuths. The magnitude spectrum at ARU (θ = 2, θ is the angle between the rupture direction and the station) and BGCA (θ = 194) seems to provide evidence for a frequency directivity effect. The maximum spectral magnitude and the radiated energy at stations in the forward rupture direction are higher than the values at stations in the backward direction. The apparent rupture time (2 × corner period) is equal to 10.74 s in the forward rupture propagation directions while the backward directions have longer rupture time of about 23.83 s. The value of the rupture velocity can be estimated from the total rupture duration in the backward direction which represents the rupture time or the apparent rupture duration as explained by Lay and Wallace (1995) using the following relation:

$$\Delta t(\theta) = \frac{L}{V_r} - \frac{L}{\beta}\cos\theta \tag{14}$$

where L is the rupture length, V_r is the rupture velocity and β is the shear wave velocity and θ is the directivity angle between strike direction and station azimuth. Using a shear wave velocity of 3.4 km/s and the rupture length of about 39 km, we obtained a rupture velocity (V_r) of 3.1 km/s that is similar to the value (3 km/s) obtained by Klinger et al. (1999).

The ARU magnitude spectrum is distorted in the transition period from 4 to 9 seconds and has higher amplitudes at the intermediate periods compared to the magnitude spectrum of BGCA which shows a clear depletion at the

Table 9. Estimated average spectral magnitude, maximum observed spectral magnitude, corner periods T_0, T_C, T_S and the rupture complexity of the Gulf of Aqaba, 1995 earthquake.

St. Code	Az.	Δ°	Aver. m_f	m_f	E_p (10^{11} J)	T_0 (sec)	T_C (sec)	T_S (sec)	C
COL	1.10	86.3	6.93	7.38	11.10	4.80	04.99	03.34	1.49
ARU	24.60	32.3	6.71	7.50	07.90	6.68	04.80	08.17	0.59
TLY	44.90	55.0	6.84	7.27	05.50	5.28	07.56	04.00	1.84
HIA	45.60	65.4	6.72	7.37	04.50	5.12	04.50	07.90	0.65
INCN	55.50	74.3	6.96	7.52	10.26	4.82	03.31	05.65	0.59
WMQ	55.40	44.0	7.11	7.64	10.70	5.27	05.46	07.27	0.75
LZH	63.50	57.5	6.71	7.35	09.36	5.27	04.89	03.48	1.14
ENH	68.30	63.7	6.82	7.51	10.59	5.06	05.30	06.42	0.82
TATO	69.60	75.6	7.03	7.70	22.60	5.27	06.50	07.20	0.91
CHTO	84.40	58.9	6.83	7.29	03.00	5.12	04.49	08.73	0.51
HYB	96.00	41.6	6.86	7.19	04.55	6.28	07.12	03.30	2.16
**KMBO*	*175.00*	*30.0*	*6.91*	*7.33*	*04.40*	*12.55*	*13.55*	*06.69*	*2.00*
**LSZ*	*189.10*	*44.5*	*6.70*	*7.20*	*02.00*	*11.15*	*09.36*	*06.42*	*1.45*
**BOSA*	*189.00*	*58.1*	*6.50*	*7.20*	*01.67*	*11.15*	*07.60*	*09.57*	*0.79*
**BGCA*	*216.00*	*38.3*	*7.03*	*7.47*	*05.10*	*12.99*	*11.40*	*11.19*	*1.01*
**DBIC*	*247.00*	*43.3*	*6.67*	*7.20*	*02.95*	*11.15*	*07.19*	*05.50*	*1.30*
**KOG*	*273.40*	*85.3*	*6.60*	*7.23*	*05.50*	*11.15*	*05.17*	*03.04*	*1.50*
MDT	286.00	33.9	6.54	7.23	01.42	5.28	06.94	13.14	0.49
PAB	299.00	33.8	6.69	7.44	04.10	5.28	07.45	11.77	0.63
MM02	314.90	83.3	6.80	7.50	08.68	4.82	05.26	07.49	0.70
GRA1	325.00	27.5	7.18	7.50	11.30	5.62	07.89	03.83	2.05
DPC	332.0	35.0	6.98	7.58	11.10	5.62	06.80	08.40	0.81
KEV	359.90	41.2	7.03	7.31	05.70	5.62	07.10	04.69	1.51
Aver. (N)			6.78 ±	7.43 ±	7.71 ±	5.37 ±	5.66 ±	6.80 ±	1.12 ±
SE			0.04	0.04	0.81	0.11	0.32	0.56	0.11
S.D.			0.17	0.15	3.36	0.50	1.32	2.80	0.53
Aver. (S)			6.70 ±	7.27 ±	6.04 ±	11.69 ±	9.82 ±		
SE			0.80	0.04	1.46	0.35	1.17		
S.D.			0.2	0.11	3.59	1.29	2.66		

Parameters symbols are as in Table 3. Aver. (N), is the average value of the source parameter of the stations to the north of 1995 earthquake epicenter while Aver. (S) is the average value of the station to the south of the epicenter (stations annotated by star).

Table 10. Source parameters derived from T_0 and T_C of the of the Gulf of Aqaba, 1995 earthquake.

Sta. Code	Parameters based on T_0				Parameters based on T_C			
	M_0 (10^{17} Nm)	L (km)	D (m)	$\Delta\sigma$ (MPa)	M_0 (10^{17} Nm)	L (km)	D (m)	$\Delta\sigma$ (MPa)
COL	06.89	20.60	0.77	2.76	07.16	21.41	0.74	2.55
ARU	13.00	28.70	0.72	2.00	09.00	20.61	1.01	3.60
TLY	05.98	22.60	0.54	1.77	08.40	32.44	0.38	0.86
HIA	05.94	21.98	0.58	1.96	06.31	19.31	0.80	3.06
INCM	09.55	20.69	1.05	3.78	06.56	14.20	1.53	8.00
WMQ	13.77	22.62	1.26	4.16	14.00	23.43	1.22	3.88
LZH	07.06	22.61	0.65	2.14	06.55	20.98	0.70	2.84
ENH	09.80	21.71	0.98	3.35	10.27	22.75	0.94	3.05
TATO	15.80	22.61	1.45	4.78	19.50	27.89	1.18	3.14
CHTO	04.94	21.98	0.48	1.63	05.30	19.27	0.68	2.62
HYB	06.23	26.95	0.41	1.12	07.00	30.55	0.35	0.86
**KMBO*	*15.70*	*53.86*	*0.26*	*0.35*	*17.30*	*58.15*	*0.24*	*0.31*
**LSZ*	*11.00*	*47.86*	*0.22*	*0.34*	*08.89*	*40.21*	*0.26*	*0.48*
**BOSA*	*11.00*	*47.86*	*0.22*	*0.34*	*07.21*	*32.61*	*0.31*	*0.72*
**BGCA*	*22.90*	*55.75*	*0.35*	*0.46*	*20.19*	*48.92*	*0.40*	*0.60*
**DBIC*	*10.15*	*47.86*	*0.22*	*0.33*	*06.83*	*30.90*	*0.43*	*0.81*
**KOG*	*11.13*	*47.86*	*0.23*	*0.36*	*06.17*	*22.18*	*0.59*	*1.79*
MDT	05.37	22.66	0.49	1.61	07.05	29.79	0.38	0.93
PAB	08.70	22.66	0.97	2.61	12.82	31.97	0.57	1.31
MM02	09.10	20.68	1.01	3.60	09.96	22.57	0.92	3.02
GRFO	10.01	24.10	0.86	2.65	14.90	33.86	0.61	1.34
DPC	12.80	24.12	1.05	3.18	15.40	29.18	0.85	2.17
KEV	06.87	24.12	0.56	1.71	08.67	30.47	0.44	1.07
Aver. (N)	13.90	23.03	0.81	2.63	9.90	25.33	0.78	2.60
± SE	± 1.80	± 0.50	± 0.07	± 0.25	± 0.96	± 1.329	± 0.08	± 0.41
S.D.	7.56	2.13	0.30	1.03	4.00	5.78	0.33	1.72
Aver. (S)	13.64	50.18	0.25	0.36	11.90	38.80	0.37	0.79
± SE	± 2.02	± 0.87	± 0.02	± 0.02	± 2.48	± 5.36	± 0.05	± 0.21
S.D.	4.90	3.60	0.05	0.05	6.10	13.80	0.13	0.52

Parameters symbols are as in Table 4. Aver. (N), is the average value of the source parameter of the stations to the north of 1995 earthquake epicenter while Aver. (S) is the average value of the station to the south of the epicenter which are annotated by star.

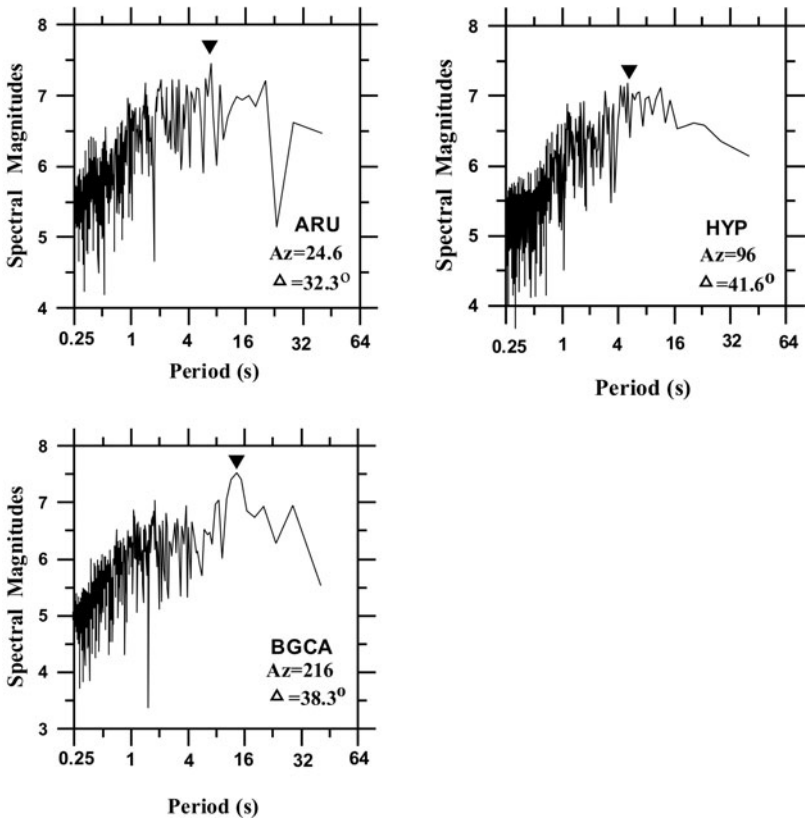

Figure 6. P-wave magnitude spectra for the November 22, 1995 Gulf of Aqaba earthquake. Plot parameters are similar to Figure (3).

higher periods. The estimated corner period at ARU is 6.7 s second shifted to 13 s at BGCA station by a directivity factor of about 1.94. The magnitude spectra for HYB station that is located nearly perpendicular to the rupture direction gives a flat magnitude spectrum level at the intermediate to higher periods. This spectral shape does not appear at the two other stations (ARU and BGCA) as expected by the model of Bernard and Herrero (1994).

Since T_0 and T_c can be used for this event we select the corner frequency T_0 due to its stability at the stations located along both sides of the rupture Table 9. Moreover, the amount of scatter is smaller for T_0 than for T_c with a relatively small standard deviation. Differences of the corner periods and maximum spectral magnitudes due to the directivity effect show also differences in the estimated source parameters. We have divided the analyzed station into two groups, one on the forward rupture direction and the other on the backward side. Table 10 shows that the estimated source parameters of the two

Table 11. Average source parameters determined from magnitude spectra of the Gulf of Aqaba 1995 earthquake considering T_0 and C.

E_P (10^{12} J)	m_f	T_c (sec)	M_0 (10^{18} Nm)	L (km)	D_0 (m)	$\Delta\sigma$ (MPa)	C	a_0/a_i	a_i (km)	D_i (m)	$\Delta\sigma_i$ (MPa)	σ_{aff} (MPa)
5.85	7.35	8.53	13.77	36.6	0.53	1.49	1.12	8.43	2.07	3..9	71.0	8.50

Parameters are as in Tables 2, 3. Where a_0, fault radius; a_i, asperity radius; s_{aff}, ambient faulting stress; D_i, dislocation associated with asperity failure; Δs_i, high stress drop released during asperity failure.

groups vary by factors of two, seven and three for the average fault lengths, stress drop and dislocation, respectively. The values of the average stress drop, average fault length and average dislocation estimated in the forward rupture propagation direction are 2.63 MPa, 23.00 km and 0.81 m, respectively. The average values of the stress drop in this direction agree well with $\Delta\sigma$ = 2.47 MPa obtained by Abdel Fattah et al. (2006) and are slightly higher than $\Delta\sigma$ = 2 MPa obtained by Pinar and Turkelli (1997) for the main rupture event. The estimated dislocation of 0.81 m in this study is in a good agreement with D_0 = 0.9 m obtained by Pinar and Turkelli (1997) while it is slightly smaller than D_0 = 1.05 m obtained by Abdel Fattah et al. (2006) for the main rupture event. Stations in the backward direction have a smaller stress drop (0.36 MPa), smaller dislocation (0.25 m) and larger fault length (50 km). The average value of the fault length obtained in this direction is in a good agreement with the estimated fault length of about 50 km from seismological data (Shamir, 1996; Pinar and Turkelli, 1997) and with the value obtained by Baer et al. (2002) from geodetic INSAR observation (~ 45–65 km).

The average seismic moment derived from the corner frequencies over different azimuths is about 13.70×10^{18} Nm, smaller than the value of 34×10^{18} Nm found by Pinar and Turkelli (1997) and the one estimated by Abdel Fattah et al. (2006) of 30×10^{18} Nm for the main rupture using the waveform inversion of the teleseismic records. The obtained rupture complexity averaged over different azimuths for this event is 1.12 and indicates a multiple complex rupture. The complexity parameters as asperity radius, displacement across the asperity, localized stress drop and ambient fault stress are also determined and listed in Table 11.

(5) The earthquake of May 18, 1998

The magnitude spectra of five broadband stations are used to determine the source parameters of this event (Tables 12, 13). The magnitude spectra are similar at the analyzed stations as shown in Figure 7 for two stations located at different azimuths. The average seismic moment calculated from T_c is 1.26×10^{17} Nm compared to 1.98×10^{17} Nm given by CMT solution and almost identical to the value of 1.24×10^{17} Nm estimated from the inversion of regional waveform

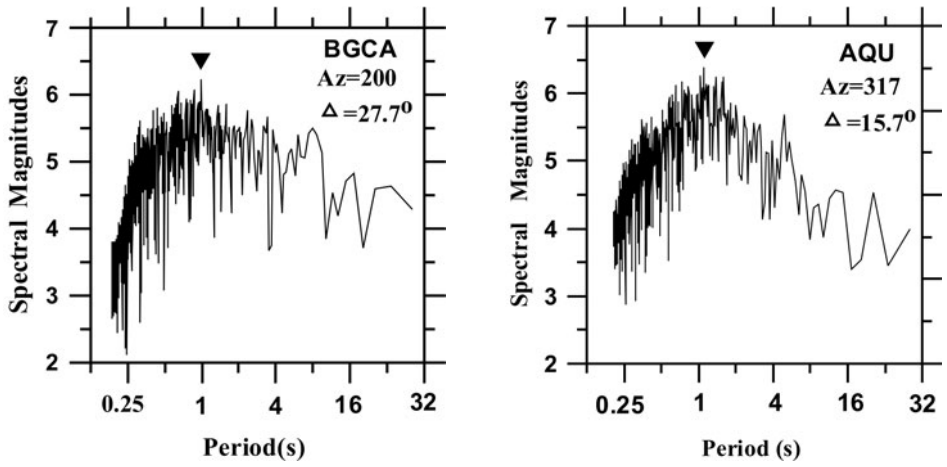

Figure 7. P-wave magnitude spectra for the May 28, 1998 Alexandria earthquake. Plot parameters are similar to Figure (3).

data (Abou Elenean and Hussein, 2007). The average stress drop is estimated to be 0.9 MPa, slightly higher than the value of 0.7 MPa obtained by Abou Elenaen and Hussein (2007). The average dislocation is 0.13 m, in excellent agreement with the value of 0.13 m obtained by Abou Elenaen and Hussein (2007). The average rupture complexity of this event is 0.41, suggesting a simple source.

5. Discussion and conclusions

In this study we have presented the average source parameters for five moderate to large size earthquakes with $5.5 \leq M_W \leq 7.3$ that have occurred since 1992 in Egypt based on the analysis of P-wave magnitude spectra of the broad band seismograms recorded at different teleseismic distances and azimuths. Inspection of the magnitude spectra of the five events indicate that both Cairo earthquake, 1992, Gulf of Aqaba earthquake, 1993 (12h:43m), its largest aftershock (16h: 33m) and Alexandria earthquake, 1998 represent relatively simple sources with simple spectra shape. On the other hand, the magnitude spectra of the Gulf of Aqaba earthquake of 1995 shows broad and complex spectra with notable differences on the estimated average source parameters related to the complexity and the NNE strong directivity of its rupture. The average values of the maximum spectral magnitudes are remarkably stable, with standard deviation less than 0.2. The visual inspection of the corner period T_0 could sometimes be influenced by site effect especially for small to moderate events with corner periods around one second. For the large events

Table 12. Estimated average spectral magnitude, maximum observed spectral magnitude, corner periods T_0, T_C, T_S and the rupture complexity of Alexandria 1998 earthquake.

St. Code	Az.	Δ°	Aver. m_f	m_f	E_p (10^{11} J)	T_0 (sec)	T_C (sec)	T_S (sec)	C
BRVK	42.10	37.4	5.18	5.88	00.86	1.55	1.89	4.37	0.43
BGCA	200.0	27.7	5.40	6.14	03.35	1.00	1.67	3.70	0.45
AQU	317.9	15.7	5.64	6.28	06.83	1.10	1.88	3.46	0.54
ECH	323.1	22.9	5.30	6.16	02.68	1.52	1.79	5.07	0.35
HGN	326.0	25.1	5.20	6.15	01.88	1.23	1.99	6.90	0.29
Aver.			5.19	6.12	3.12	1.28	1.84	4.7	0.41
			±	±	±	±	±	±	±
SE			0.08	.07	1.02	0.11	0.05	0.62	0.04
S.D.			0.19	0.15	2.27	0.24	0.12	1.38	0.10

Parameters are as in Table 3.

Table 13. Source parameters derived from T_0 and T_C of Alexandria 1998 earthquake.

Station	Parameters based on T0				Parameters based on TC			
	M_0 (10^{17} Nm)	L (km)	D (m)	$\Delta\sigma$ (MPa)	M_0 (10^{17} Nm)	L (km)	D (m)	$\Delta\sigma$ (MPa)
BRVK	05.80	6.65	0.06	0.70	07.09	8.11	0.05	0.46
BGCA	06.80	4.29	0.17	3.03	11.41	7.17	0.11	1.08
AQU	10.40	4.72	0.22	3.45	17.70	8.07	0.13	1.18
ECH	10.90	6.52	0.12	1.37	12.80	7.68	0.10	0.99
HGN	08.60	5.28	0.15	2.08	13.90	8.54	0.09	0.78
Aver.	08.50	5.49	0.14	2.13	12.58	7.91	0.10	0.90
	±	±	±	±	±	±	±	±
SE	1.00	0.48	0.03	0.50	1.74	0.23	0.01	0.13
S.D.	2.21	1.06	0.06	1.14	3.86	0.52	0.03	0.29

Parameters are as in Table 4.

with corner period larger than three seconds, T_0 and T_c are close to each other. For earthquakes with complex rupture and strong directivity the corner periods are azimuthaly dependent. The uniform stations distribution over different azimuths is important in order to obtain reliable and more accurate values of the source parameters.

The magnitude spectra for the 1995 Gulf of Aqaba earthquakes show that there is a large difference in the shape of the spectrum together with the cor-

ner periods in addition to the parameters describing the source at the stations in the forward rupture propagation direction compared with stations in the backward direction. These variations are mainly due to a rupture directivity effect. The corner periods averaged for different azimuths indicate that the rupture propagates from the south to the north of the Gulf of Aqaba. The shape and the duration of the source time function for each station obtained by the inversion technique for the 1995 Gulf of Aqaba earthquake reflect the same direction of propagation (Klinger et al., 1999 and Gitterman et al., 1996 a). The appearance of rupture directivity at periods longer than 4 for this event indicates that the rupture directivity effect of large earthquakes may be more pronounced at longer periods. The average value of the moment for the main rupture in this study is smaller than the values of moment estimated in the previous work using the inversion technique. This is mainly due to the complexity of the source which consists of two subevents (Pinar and Turkelli, 1997 and Hofstetter et al., 2003) or three subevents (Abdel Fattah et al., 2006). The superposition of the time histories of these subevents may become incoherent and consequently the interference will not be constructive and the resulting spectrum plateau is the RMS of the point source spectral plateaus (e.g. Frankel, 1991), independently of the direction of the rupture propagation. Therefore, the values of the moment will be underestimated. However, the obtained value of the moment for the main rupture of this event in the previous studies is in agreement with our determination within a factor of 2.5. This factor lies within the usually uncertainty of the moment determination (Hanks and Wyss, 1972). The rupture complexity parameter *C* for 1995 Gulf of Aqaba earthquakes suggests a complex event with extremely high local stress drop in a smaller asperity area, about 50 times larger than the average stress drop over the fault whereas the August 3, 1993 event and its aftershock suggest a smooth simple rupture with homogeneous stress drop. This indicates that the 1995 event radiates seismic energies from a small region in a short time during the earthquake.

The magnitude spectra of August 3, 1993 main shock shows a relatively long corner period compared to its aftershocks. This difference is reflected in the stress drop where the stress drop of the main shock is found to be larger than the value estimated from the aftershock. Such change from high to low stress drop reflects a stress relaxation in the volume under consideration (Kaiser and Duda, 1988). The stress drops of the three Gulf of Aqaba events show an increasing trend with seismic moment.

The two intraplate shocks; 1992 Cairo earthquake and 1998 Alexandria released a high stress drop relative to the Gulf of Aqaba earthquakes of comparable size. The average stress drop of the examined five shallow earthquakes in this study are consistent with Kanamori and Brodsky (2004) results for shallower earthquakes with stress drop in the range of 1 to 10 Mpa. The correlation between the stress drop and the moment magnitude shows no simple relation that may be related to the different tectonic environment.

Aknowledgement – We thank Prof. S. J. Duda, Hamburg University, for his valuable advice and reviewing the manuscript.

References

Abou Elenean, K. M. (2007): Focal mechanisms of small and moderate size earthquakes recorded by the Egyptian National Seismic Network (ENSN), Egypt, *NRIAG J. Geophys.*, 6, No. 1, 119–153.

Abou Elenean, K. M. and Hussein, H. M. (2007): Source mechanism and source parameters of May 28, 1998 earthquake, Egypt, *J. Seismol.*, **11**, 259–274.

Abdel Fattah, A. K. (1996): Rupture process characteristics of August 1993 Aqaba earthquake sequence, Ph. D thesis. Faculty of Science, Ain Shams University, Cairo. Egypt

Abdel Fattah, A. K., Hussein, H. M. and El Hady, S. (2006). Another look at the 1993 and 1995 Gulf of Aqaba earthquake from the analysis of teleseismic waveforms. *Acta Geophys.*, **54**, No.3, 260–279.

Aki, K. (1967): Scaling low of seismic spectrum. *J. Geophys. Res.*,**72**, 1217–1231.

Andrews, D. J. (1986): Objective determination of source parameters and similarity of earthquakes of different size. In Das, S., Boatwright, J. and Scholz, C. H. (Eds): *Earthquake source mechanism*. Geophysical Monograph 37, Maurice Ewing, 6, Geophys. Un., Wash. D. C., 259–267.

Andrews, D. J. (1986): *Objective determination of source parameters and similarity of earthquakes mechanics*. Geophysical Monograph 37, Maurice Ewing, 6, Geophys. Un., Wash. D. C., 259–267.

Baer, G., Shamir, G., Sandwell, D. and Bock, Y. (2002): Crustal deformation during 6 years spanning the Mw 7.2 1995 Nuweiba (InSAR), *Isr. J. Earth Sci.,* **50**, 9–22.

Bernard, P. and Herrero, A. (1994): Slip heterogeneity, body-wave spectra, and directivity of earthquake ruptures. *Ann. Geofis.*, XXXVII, **6**, 1679–1690.

Boatwright, J. (1980): A spectral theory for circular seismic sources; simple estimates of source dimension, dynamic stress drop, and radiated seismic energy, *Bull. Seism. Soc. Am.*, **70**, 1–27.

Boatwright, J. (1984): The effect of rupture complexity on estimates of source size, *J. Geophys. Res.*, **89**, 1132–1146.

Boore, D. M. and Boatwright, J. (1984): Average body wave radiation coefficients, *B. Seismol. Soc. Am.*, **94**, 1615–1621.

Brune, J. N. (1968): Seismic moment, seismicity and the rate of slip along major fault zones. *J. Geophys. Res.*, **73**, 777–784.

Brune, J. N. (1970): Tectonic stress and the spectra of seismic shear waves from earthquakes, *J. Geophys. Res.*, **75**, 4997–5009.

Brune, J. N. (1971): Correction, *J. Geophys. Res.*, **76**, 5002.

Duda, S. J. and Kaiser, D. (1989): Spectral magnitudes, magnitude spectra, and earthquake quantification; The stability issue of corner period and the maximum magnitude for a given earthquake. *Tectonophysics*, **166**, 205–219.

Frankel, A (1991): High frequency spectral fall-off earthquakes, fractal dimension of complex rupture, b value, and the scaling strength of faults. *J. Geophys. Res*, **96**, 6291–6302.

Gitterman, Y., Shapira, A. and Peled, U. (1996): Analysis of strong motion records of the 22.11.95 Nuweiba earthquake and its aftershocks, Israel Geological Society Annual Meeting, Eilat, Abstracts, p. 33.

Hanks, T. C. (1982): Reply to comments on žthe corner frequency shift, earthquake source models and Q'. *B. Seismol. Soc. Am.*, **72**, 1433–1445.

Hanks, T. C. and Wyss, M. (1972): The use of body wave spectra in determination of seismic source parameters. *B. Seismol. Soc. Am.*, **62**, 561–589.

Hofstetter, A., Thio, H. and Shamir, G. (2003): Source mechanism of the 22/11/1995 Gulf of Aqaba earthquake and its aftershock sequence, *J. Seismol.*, **7**, 77–114.

Hussein, H. M. (1999): Source process of the October 12, 1992 Cairo earthquake. *Ann. Geofis.*, **42**, 4, 665–647.

Hussein, H. M., Abou Elenean, K. M., Ibrahim, E. M., Ahmed S. Abou El Atta and Duda, S. J. (1998): Spectral magnitudes and source parameters for some damaging earthquakes in Egypt. *Bull. IISEE*, V. **32**, 1–16.

Kaiser, D. (1989): Seismizität des Erdkörpers: Magitudenspektren und andere Erdbeben-Herdparameter aufgrund von Breitband-Seismogrammen. Ph.D.-Thesis, Universität Hamburg.

Kaiser, D. and Duda, S. J. (1988) Magnitude spectra and other source parameters for some major 1985 and 1986 earthquakes. In Kulhanek, O. (Ed.): Seismic source physics and earthquake prediction research, *Tectonophysics*, **152**, 203–218.

Kaiser, D., Duda, J. S. and Chowdhury, D. K. (1996): P-wave magnitude spectra, stress drops, rupture complexities and other source parameters from broadband seismograms of three 1987 Southern California earthquakes, *Geofizika*, **13**, 1–29.

Kanamori, H. and Brodesky, E. (2004): The physics of earthquakes, *Rep. Prog. Phys.*, **67**, 1429–1496.

Keilis-Borok, V. (1959): On the estimation of the displacement in an earthquake source and of source dimension, *Ann. Geofis.,* **12**, 205–214.

Klinger, Y., Rivera, L., Haessler, H. and Maurin, J. C. (1999): Active faulting in the Gulf of aqaba: new knowledge from the Mw 7.3 earthquake of 22 November 1995, *B. Seismol. Soc. Am.,* **89**, 1025–1036.

Lay, T. and Wallace, T. C. (1995): *Modern Global Seismology*. Academic Press. San Diego, 521 pp.

Madariaga, R. (1979): On the relation between seismic moment and stress drop in the presence of stress and strength heterogeneity, *J. Geophys. Res.*, **84**, 2244–2250.

McGarr, A. (1981): Analysis of Peak ground motion in terms of model of inhomogeneous faulting, *J. Geophys. Res.,* **86**, B5, 3901–3912.

Nortmann, R. and Duda, S. J., (1983): Determination of spectral properties of earthquakes from their magnitudes. In Duda, S. J. and Aki, K. (Eds): Quantifications of Earthquakes, *Tectonophysics*, **92**, 251–275.

Pinar, A. and Turkelli, N. (1997). Source inversion of the 1993 and 1995 Gulf of Aqaba earthquakes, *Tectonophysics*, **293**, 279–288.

Riad, S. and Meyers, H. (1985): *Earthquake catalog for the Middle East Countries 1900–1983*. World Data Center for Solid Earth Geophysics, Rep. SE–40, National Oceanic and Atmospheric Administration (NOAA),US Dept. of Commerce, Boulder, Colorado, USA.

Roslov, Y. (1994): Program for amplitude spectrum treatment and analysis, *Acta Geophys. Polonica*, XL **11**, 4, 315–319.

Sarkar, D. and Duda, S. J. (1985): Spectral P-wave magnitudes, Aki's omega-square model and source parameters of earthquakes, *Tectonophysics*, **188**, 175–193.

Shamir, G. (1996): The November 22, 1995, Nuweiba Earthquake, Gulf of Elat (Aqaba): mechanical analysis, IPRG Rep., 550/87/96.

Snoke, J. A. (1987): Stable determination of (Burne) stress drops, *B. Seismol. Soc. Am.,* **77**, 530–538.

Zwillinger, D. (1995): CRC Standard Mathematical Tables and Formulae, Boca Raton (Eds.), FL: CRC Press.

SAŽETAK

Parametri izvora za značajne potrese u Egiptu (1992–1998), određeni iz magnitudnog spektra P-valova širokopojasnih seizmograma dalekih potresa

H. M. Hussein i K. M. Abou Elenean

Koristeći magnitudni spektar P-valova vertikalne komponente širokopojasnih seizmograma dalekih potresa, određeni su prosječni parametri izvora za pet značajnih potresa s magnitudama Mw ≥ 5.7 koji su se dogodili u Egiptu (potres kod Kaira iz 1992, Aleksandrije 1998. i tri potresa u zaljevu u Aqaba regiji između 1993. i 1995.). Magnitudni spektar predstavlja spektar gustoće amplitude brzine u izvoru potresa, iskazan u jedinicama magnitude. Za procjenu parametara izvora korišten je maksimum magnitudnog spektra te period na kojem je opažen maksimum. Kritični period određen je pomoću dvije metode. Dobiveni parametri uspoređeni su s onima koji su izvedeni u prethodnim studijama. Rezultati pokazuju da u području magnituda 5,5 ~ 7,2 kritični periodi iznose 1,29 ~ 11,6 s, duljine rasjednih pukotina 5,5 ~ 50 km i pad napetosti od 0,5 ~ 4,8 MPa. Za tri potresa u zaljevu Aqaba pad napetosti pokazuje trend povećanja sa seizmičkim momentom. Potres iz 1995. u zaljevu Aqaba magnitude Mw = 7,2, najjači potres koji se u prošlom stoljeću dogodio u Egiptu, složeniji je u odnosu na druge potrese. Kritični period ovog potresa ovisan je o azimutu zbog složenosti i izražene usmjerenosti pucanja rasjeda. Za potres iz 1995. procijenjeni su i dodatni parametri izvora u smislu modela nehomogenog izvora. Ti parametri su radijus zone početnog rasjedanja, pomak duž nje, lokalni pad napetosti te okolna napetost rasjedanja. Prosječni pad napetosti za potrese u Kairu 1992. i Alexandriji 1998. veći je nego za potres u zaljevu Aqaba 1993. Procijenjeni seizmički moment dobiven upotrebom magnitudnog spektra uz pretpostavku jednostavnog izvora dobro se podudara s procjenama pomoću drugih metoda, dok pretpostavljeni složeniji izvor daje manje vrijednosti.

Ključne riječi: magnitudni spektar, parametri izvora, složenost izvora

Corresponding author's address: H. M. Hussein, Seismology Department, National Research Institute of Astronomy and Geophysics, El marsad St. Helwan 11421, Egypt, tel: 202–25583887, fax: 202–25548020, e-mail: hesham6511421@yahoo.com